JACS
JOURNAL OF THE AMERICAN CHEMICAL SOCIETY

ARTICLE

pubs.acs.org/JACS

Can Amorphous Nuclei Grow Crystalline Clathrates? The Size and Crystallinity of Critical Clathrate Nuclei

Liam C. Jacobson and Valeria Molinero*

Department of Chemistry, University of Utah, 315 South 1400 East, Salt Lake City, Utah 84112-0850, United States

ABSTRACT: Recent studies reveal that amorphous intermediates are involved in the formation of clathrate hydrates under conditions of high driving force, raising two questions: first, how could amorphous nuclei grow into crystalline clathrates and, second, whether amorphous nuclei are intermediates in the formation of clathrate crystals for temperatures close to equilibrium. In this work, we address these two questions through large-scale molecular simulations. We investigate the stability and growth of amorphous and crystalline clathrate nuclei and assess the thermodynamics and kinetic factors that affect the crystallization pathway of clathrates. Our calculations show that the dissociation temperature of amorphous clathrates is just 10% lower than for the crystals, facilitating the formation of metastable amorphous intermediates. We find that, at any temperatures, the critical crystalline nuclei are smaller than critical amorphous nuclei. The temperature dependence of the critical nucleus size is well described by the Gibbs−Thomson relation, from which we extract a liquid-crystal surface tension in excellent agreement with experiments. Our analysis suggests that at high driving force the amorphous nuclei may be kinetically favored over crystalline nuclei because of lower free energy barriers of formation. We investigated the role of the initial structure and size of the nucleus on the subsequent growth of the clathrates, and found that both amorphous and sI crystalline nuclei yield crystalline clathrates. Interestingly, growth of the metastable sII crystal polymorph is always favored over the most stable sI crystal, revealing kinetic control of the growth and indicating that a further step of ripening from sII to sI is needed to reach the stable crystal phase. The latter results are in agreement with the observed metastable formation of sII CO_2 and CH_4 clathrate hydrates and their slow conversion to sI under experimental conditions.

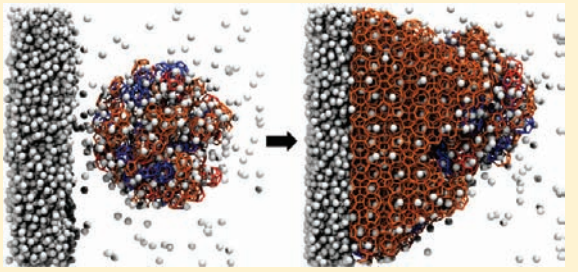

INTRODUCTION

Clathrate hydrates are crystals in which hydrogen-bonded water networks form polyhedral cages that enclose nonpolar molecules such as methane and carbon dioxide. Clathrates occur naturally and in great abundance on the sea floor, and are the most abundant source of fossil fuels on our planet.[1] The crystallization of clathrate hydrates is of utmost importance in a wide range of applications, from the prevention of clogging in oil and gas pipelines to the safe transportation of natural gas from remote resources.[2] Methods to promote and prevent the formation of clathrate hydrates are of significant importance to scientists and engineers. Therefore, there is great interest in understanding the mechanism of hydrate nucleation, and the nature of the nascent clathrate nuclei.

State of the art experimental techniques are not yet able to resolve and characterize the structure of clathrate nuclei.[3] Some insights on the structure of clathrate nuclei, however, have been obtained from molecular simulations.[4−7] These are typically carried out under conditions of high driving force such as supercooling the system with respect to the clathrate phase or supersaturating the solution with guest molecules. Such simulations at high driving force result in the formation of amorphous clathrate structures.[4−7] These amorphous clathrates are made of the same polyhedral cage building blocks of the crystalline clathrates, but lack their long-range order. In a previous simulation study, we have shown that the nucleation of clathrate hydrates in supercooled conditions takes place through a multistep mechanism involving amorphous precursors.[6] The same mechanism has been observed by Vatamanu et al. using different model and simulation methodology.[7] These results are in contrast to classical nucleation theory that states that the nucleation of the crystalline phase takes place through a building up of monomers already arranged with the symmetry of the crystal phase.

The "blob mechanism" of clathrate crystallization proposed in ref 6 involves first the creation from the dilute solution of a blob: an amorphous cluster of solvent-separated guest molecules with interstitial water that continually rearranges to form *transient* clathrate cages. If the blob intermediate is sufficiently large and long-lived, the water molecules surrounding the solvent-separated guests form *persistent* polyhedral cages resulting in an amorphous clathrate intermediate that is able to nucleate the growth of the crystalline clathrate phase. Similar multistep mechanisms have been proposed for the crystallization of proteins and colloids: a sequence of steps that include first the densification from a dilute phase into a dense amorphous intermediate and subsequent ordering of the dense intermediate into a more stable

Received: February 14, 2011
Published: April 05, 2011

dx.doi.org/10.1021/ja201403q | *J. Am. Chem. Soc.* 2011, 133, 6458–6463

crystal.[8,9] Ten Wolde and Frenkel modeled globular proteins using Lennard-Jones particles with attractive, short-ranged interactions and discovered that the dilute fluid phase has a fluid−fluid coexistence curve with the dense amorphous phase that is metastable to the dilute fluid-crystal coexistence curve.[10] Below the fluid−fluid coexistence line, the free energy of the dense, disordered intermediate phase is lower than for the solution. Above this coexistence line, the intermediate is metastable to both the dense disordered and ordered phases.[11] Recent work involving simulations of protein crystallization indicates that the dense disordered phase might still be an intermediate above the fluid−fluid coexistence line where the dense amorphous phase is unstable.[9,12] These results suggest that amorphous intermediates might form in the nucleation pathway, even under conditions of low driving force. Therefore, it is important to understand the properties that such amorphous nuclei might have as well as whether and how the amorphous clathrates might be able to grow the crystal phase.

The formation of amorphous clathrates in simulations at high supercooling indicates that they are stable with respect to the solution under these conditions. A first question addressed in this study is whether there are temperatures for which the amorphous clathrate is more stable than the crystal. We compute the dissolution (i.e., melting) temperatures of amorphous and crystalline clathrates and determine the size of their respective critical nuclei as a function of temperature. We further investigate whether there could be conditions for which the amorphous clathrate nuclei are favored not by thermodynamics but by a lower free energy of formation from the solution. A second question we address is whether amorphous clathrate nuclei can grow into crystalline clathrates by either reorganization of the amorphous network or by growth of a crystalline phase around an amorphous seed. Answering this question is key to determine the feasibility of a multistep mechanism of clathrate crystallization involving amorphous clathrate nuclei.

The nucleation of clathrates in simulations is a rare event, and the time scales and computational resources needed to observe nucleation at low driving force are immense. Thus in this work we focus on the stability and growth of premade amorphous and crystalline nuclei, and not on their initial formation from the solution. A second challenge arises from the growing size of the critical nuclei on decreasing the driving force, requiring large-scale simulation cells that would make this study computationally very expensive with the use of atomistic models. We surpass this challenge through the use of a coarse-grained model of water and a methane-like guest that accurately describes the thermodynamics of clathrate formation and the mechanisms of nucleation and growth from solution, and it is 2−3 orders of magnitude computationally more efficient than fully atomistic atomistic models.[6,13−15]

METHODS

Force Fields. Water was modeled using the monatomic water model mW.[16] The guest, that we call M here and in refs 6 and 14, is also represented by a single particle with properties intermediate between methane and carbon dioxide.[13] The melting temperatures of sI and sII clathrate hydrates of the M guest, along with structural and thermodynamic properties of these crystals and the M-water solutions were presented and validated in refs 6, 13, and 14.

Simulations. Molecular dynamics simulations were carried out with LAMMPS.[17] The equations of motion were integrated with the velocity Verlet algorithm using 10 fs time steps.[16] Simulations were performed in the isothermal−isobaric (NpT) ensemble using the Nose−Hoover thermostat and barostat with damping constants 1 and 5 ps, respectively. All simulations were performed at pressure of 50 MPa. Periodic boundary conditions were used in the three dimensions.

Systems. A 128 Å × 128 Å × 128 Å simulation cell (54,000 molecules) of bulk sI clathrate crystal with all cages occupied by single M guests was equilibrated at T = 270 K and p = 50 MPa. Approximately spherical crystalline clathrate clusters were constructed by freezing the positions of the water and guest molecules within 10, 15, 20, 25, and 30 Å of the center of the equilibrated lattice and melting the rest of the molecules, after transforming them all to water. A slab of water particles of the liquid was converted to M particles, and equilibrated at 300 K and 50 MPa for 10 ns, resulting in a three phase system: a slab of M liquid in contact with a water solution saturated with M containing a solid clathrate nucleus. The solubility of M in water is 0.0038 mol fraction at 178 atm and 313 K, intermediate between the one of methane, 0.0023, and carbon dioxide, 0.024, under the same conditions.[13] Amorphous clathrate nuclei of initial radii 10, 20, and 30 Å were obtained in a similar fashion, selecting spherical regions from the last configuration of a deeply supercooled simulation[14] in which a water-guest solution produced an amorphous clathrate solid. Guest molecules were placed in the center of mass of all clathrate cages.

We considered a single amorphous nucleus for each radius R. While the amorphous clathrates do not have a unique structure, we previously demonstrated that the percentage of each cage type ($5^{12}6^n$ with n = 0, 2, 3 and 4) in the amorphous clathrates is constant across different simulations.[14] Thus, we expect that due to self-averaging of different local structures, amorphous nuclei of radius R prepared from distinct simulation runs would result in the same thermodynamic properties. The excellent fit of the amorphous dissociation temperature data to the Gibbs−Thomson (GT) equation, and the agreement between the bulk value of melting temperature obtained from the GT equation and the direct determination from the bulk simulations, both presented in the Results and Discussion section below, strongly suggests that the self-averaging of the amorphous structures is valid down to the smallest nucleus size considered in this study.

Thermodynamic Data. The melting temperatures (T_m) for bulk crystalline sI and sII clathrates with the M guest at p = 50 MPa were determined in a previous study.[6] The T_m for the spherical nuclei of the crystalline sI and amorphous clathrates as well as the bulk amorphous clathrate were determined using the method of direct coexistence with the protocols detailed in ref 13. Phase coexistence simulations were repeated in steps of 5 K. Simulation times of up to 100 ns were needed to observe the advance of crystallization or dissolution of the system.

As the nuclei can be modified during their initial pre-equilibration with the solution, the sizes of nuclei used for the melting point determinations were measured in terms of the number of guest molecules N_g that belonged to each clathrate cluster after the equilibration process indicated above. N_g was determined by identifying the solvent-separated guest molecules that belonged to the same cluster. The effective radius of the cluster R is obtained by using the average number density of guests in the clathrate lattice $\rho = N_g/V$, where $V = (4/3)\times\pi R^3$ is the volume of a sphere, resulting in R = 0.365 nm × $(N_g)^{1/3}$ for the crystalline nuclei and R = 0.43 nm × $(N_g)^{1/3}$ for the amorphous nuclei.

The enthalpy of dissociation or melting ΔH_m per mole of water was calculated by subtracting the enthalpy of liquid water and the enthalpy of the guest from the enthalpy of the clathrate using the appropriate stoichiometry. The entropy of dissociation was determined as $\Delta S_m = \Delta H_m/T_m$. The enthalpy for the amorphous phase was determined by calculating the enthalpy $\langle H\rangle = \langle E + pV\rangle$, normalized per mole of water, of a system of amorphous clathrate. Since not all the water was converted to amorphous clathrates during their formation,[14] the enthalpy of the

Table 1. Thermodynamic Properties of Bulk Amorphous and sI Crystalline Clathrates

property	amorphous	crystalline	amorphous/crystalline
T_m (K)[a]	276 ± 6	307 ± 2	0.90
T_m (K)[b]	281	300	0.94
ΔH_m (kJ/mol)[c]	5.40	6.53	0.83
ΔS_m (J/K mol)[c]	19.8	21.3	0.93
K_{GT} (K nm)	34.8	36.6	0.95
γ (mJ/m^2)	<32	36	--

[a] Computed from phase coexistence method of bulk slabs. [b] Determined from Gibbs−Thomson relation (eq 1). [c] Normalized per mole of water.

N_w "non-clathrate" water molecules present in the amorphous clathrate simulation cell but that did not belong to any clathrate cages was subtracted as that of liquid water: $\langle H\rangle_{amorphous} = \langle H\rangle_{system} - \langle H\rangle_{non\text{-}clathrate\ water}$, where $\langle H\rangle_{non\text{-}clathrate\ water}$ is determined from simulations of liquid water under the same conditions $\langle H\rangle_{non\text{-}clahtrate\ water} = N_w \langle H\rangle_{water}$, $\langle H\rangle_{water}$ is the enthalpy of liquid water.

RESULTS AND DISCUSSION

The stable phase of the M clathrate hydrate is, same as for CH_4 and CO_2 clathrates, the sI crystal, with a melting temperature $T_m^X = 307 \pm 2$ K.[14] The sII crystal is metastable to sI but close in free energy, with a melting temperature 303 ± 1 K.[14] We find that the melting temperature of the amorphous clathrate is about 90% of the melting temperature of the crystal, $T_m^A = 276 \pm 6$ K. Interestingly, the ratio between T_m^A and T_m^X is almost the same as found for the stable liquid-crystal and metastable liquid−liquid equilibrium in the crystallization of lysozyme, a protein that −as the clathrates− presents a multistep mechanism of crystallization assisted by a dense but disordered amorphous phase.[11]

Table 1 shows the interplay between entropy and enthalpy on the relatively high stability of the amorphous clathrate. The amorphous clathrate has higher entropy than the crystal, favoring its formation from the liquid. The enthalpies of melting for the amorphous and crystalline clathrates are close (5.4 and 6.5 kJ/mol; Table1), with values comparable to the those for the melting for ice (5.3 kJ/mol[16]) and the empty clathrate (4.4 kJ/mol[15]). These results indicate that the enthalpies of all these phase transitions are dominated by the ordering of liquid water to form a fully hydrogen-bonded network.

In the nucleation of a new phase, nuclei that are smaller than the critical size dissolve and those that are larger grow. We determined the size of the critical clathrate nuclei through the computation of the dissolution temperature of premade spherical nuclei: for a given temperature T the critical radius R is the one for which its melting point $T_m(R)$ equals T. Figure 1 presents the melting temperatures for the crystalline and amorphous nuclei as a function of their radii R and their respective fits to the Gibbs−Thomson equation for spherical particles,

$$T_m(R) = T_m^{bulk} - \frac{2K_{GT}}{R} \qquad (1)$$

The Gibbs−Thomson constant is $K_{GT} = T_m^{bulk}\gamma v/\Delta H_m$, where γ is the liquid−solid surface tension, v is the molar volume and ΔH_m is the bulk enthalpy of melting. Equation 1 gives a very good description of the data (correlation coefficient above 0.998) and predicts values for T_m of the bulk phases, $T_m^A = 281$ K and $T_m^X = 300$ K, in excellent agreement with those determined from the direct phase coexistence method. For any temperature, we find that the critical size for crystalline nuclei is smaller than for amorphous nuclei, with the two becoming essentially indistinguishable in terms of stability for nuclei with less than 15 guest molecules, a size comparable to the unit cell of the clathrate.

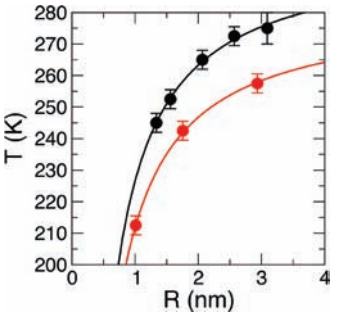

Figure 1. Melting or dissociation temperature of crystalline (black) and amorphous (red) nuclei as a function of their radius. The lines are the fits with the Gibbs−Thomson relation (eq 1) with the parameters of Table 1, and indicate the critical nucleus size R for each temperature T. According to classical nucleation theory, the radius of the critical nucleus is $R^*(T) = -2\gamma/(\Delta\mu(T)\rho_l) \approx 2\gamma/(\rho\Delta S_m(T_m^{bulk} - T))$. The coarse-grained model predicts correctly γ but underestimates the experimental ΔS_m by about 20%, because the monatomic it cannot account for the increase in rotational entropy of the water and guest on melting.[13] Thus, for a given supercooling $T_m^{bulk} - T$ the radii of the critical nuclei would be about 20% smaller than predicted by the simulations.

The Gibbs−Thomson constants we obtained for the amorphous and crystalline clathrates are $K_{GT}^A = 34.8$ K nm and $K_{GT}^X = 36.6$ K nm. These are comparable to the value for ice, 26 K nm as determined from experimental thermodynamic data.[18] When comparing to results from the literature, it is important to note that some authors include the factor of 2 from eq 1 in the definition of K_{GT}. The mW water model used in this study accurately predicts[19] the freezing point depression of water confined in cylindrical nanopores measured in cryoporometry[20] and calorimetry[21] experiments.

Using K_{GT}, bulk T_m, ΔH_m, and molar volume of the hydrate, we determined the surface tensions between liquid and sI crystal, $\gamma_x = 36 \pm 2$ mJ/m^2. The surface tension determined from the simulations is in excellent agreement with those determined from the experimental melting temperatures of CH_4 and CO_2 clathrates in cylindrical pores of various radii. Anderson et al. determined the experimental water-sI CH_4 and CO_2 clathrates interfacial energies by measuring hydrate equilibria in mesoporous silica.[22] They obtained surface tensions γ equal to 32 ± 3 and 30 ± 3 mJ/m^2 for CH_4 and CO_2 clathrate−water interfaces, respectively. Using the same methods, they determined γ for the ice−water interface to be 32 ± 2 mJ/m^2. Uchida et al. obtained clathrate−water surface tension values of 17 ± 3 and 14 ± 3 mJ/m^2 for CH_4 and CO_2 clathrate-water interfaces, respectively.[23] Anderson et al. recalculated the values using the experimental results of Uchida et al., but accounting for the correct hysteresis conditions and obtained values of 34 ± 6 mJ/m^2 and 28 ± 6 mJ/m^2 for CH_4 and CO_2 clathrate-water interfaces, respectively.[22]

The same analysis employed for the crystal could be used to estimate the surface tension of the amorphous nuclei. We note, however, that the amorphous nuclei used in this study are porous and not fully filled with clathrate cages, thus they effectively have a considerable larger exposed liquid−solid area than expected for a perfect sphere. This implies that the surface tension predicted

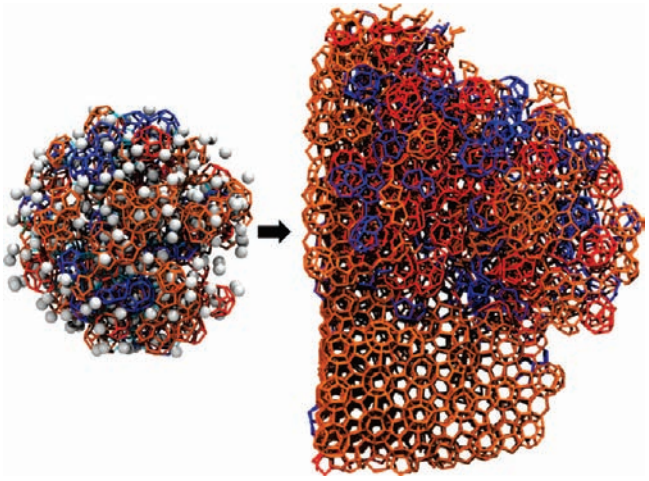

Figure 2. Amorphous nucleus with R = 30 Å at the beginning of the simulation (left) and after 100 ns of growth (right) at T = 250 K. The nucleus at the beginning of the simulation had 2128 water molecules that belonged to a polyhedral clathrate cage. Of those, 20% were identified as being sI (shown in blue) and 50% were identified as being sII (shown in orange). Cages shown in red correspond neither to the sI or sII structure. Although initially there were no large crystalline domains of any of the two crystals, the amorphous nucleus grew a crystalline clathrate. After 100 ns of growth, there were 10438 water molecules in polyhedral cages. Of those, 12% were identified as sI and 64% were identified as sII. Guest molecules (white balls) have been omitted from the final structure so that the sII crystalline lattice is clearly appreciated. The flat edge of the final structure rests on the guest-water interface, as also shown in the Abstract graphic.

from the Gibbs−Thomson constant by assumption of spherical geometry, γ_a = 32 mJ/m^2, is an upper limit to the real value for the amorphous clathrate. From the porosity of the amorphous nuclei, we estimate that the surface tension of compact amorphous clathrates could be as small as half that value. A more accurate knowledge of that surface tension would permit the estimation of the relative barriers of formation of the amorphous and crystalline nuclei from solution. According to classical nucleation theory, the free energy barrier to nucleation is

$$\Delta G^* = \frac{16\pi\gamma^3 v^2}{\Delta\mu^2} \qquad (2)$$

where $\Delta\mu = \Delta T \Delta S_m$, and $\Delta T = T_m^{bulk} - T$.[24] The ratio ζ of the free energy barriers for nucleation of the amorphous and crystalline structures would then only depend on the ratio between their solid−liquid surface tensions and the driving force

$$\zeta = \frac{\Delta G_A^*}{\Delta G_X^*} = \frac{\gamma_A{}^3 \Delta S_X{}^2 (T_m^X - T)^2}{\gamma_X{}^3 \Delta S_A{}^2 (T_m^A - T)^2} \qquad (3)$$

Nucleation of clathrates in simulations at temperatures up to as high as ∼20% supercooling start with amorphous nuclei.[4−6,14,25−28] This suggests that although the amorphous critical nuclei are larger than the crystalline nuclei for any temperature, their formation may be kinetically favored by lower free energy barriers. Equation 2, along with the data of Table 1, indicates that formation of amorphous nuclei could be kinetically favored up to 255 K (17% supercooling) if γ_a/γ_x were 0.5 and up to 230 K (25% supercooling) if the ratio of the surface tensions were 0.66). For these estimations, we used the melting temperatures of sI and amorphous clathrates obtained by the phase-coexistence

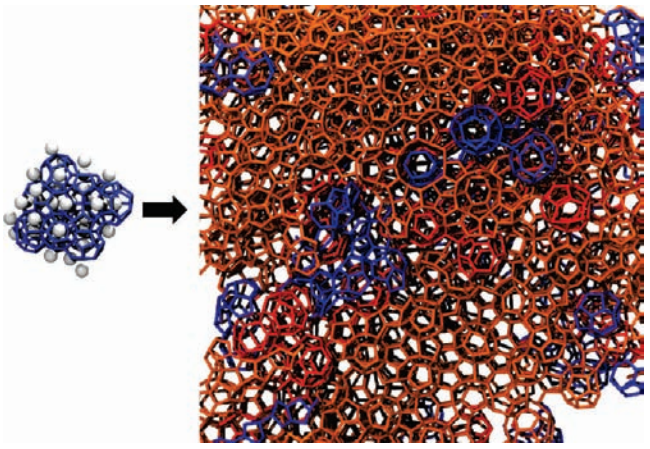

Figure 3. Crystalline sI nucleus with R = 10 Å at the beginning of the simulation (left) and after 100 ns of growth (right) at T = 240 K. The domains of sI clathrate are identified in blue and the domains of sII clathrate are colored orange. Guest molecules (white balls) have been omitted from the final structure for clarity.

method; the $T_m{}^x$ and $T_m{}^A$ predicted by the extrapolation of the Gibbs−Thomson equation are closer, predicting an even larger temperature range for which nucleation through amorphous clusters would be kinetically favored. Further work is needed to more accurately assess the interfacial energies of compact amorphous nuclei.

Finally, we investigated the growth of the clathrate nuclei and the degree of crystallinity in the structures grown from amorphous and crystalline seeds. To identify the clathrate cages that belong to sI and sII domains we used order parameters developed in a separate study.[29] Each water molecule in the sI and sII lattice is the vertex of four polyhedral cages; we distinguish water molecules that belong to the sI and sII crystals by identifying the unique vertices of polyhedra present in the clathrate lattices where the polyhedral cages meet. Water molecules in the sI vertices belong to only $5^{12}6^2$ cages, or to both $5^{12}6^2$ cages and 5^{12} cages. Water in the sII vertices belong only to 5^{12} cages, or to 5^{12} and $5^{12}6^4$ cages, or to only $5^{12}6^4$ cages. These order parameters give us the ability to determine whether the amorphous nuclei lead to the formation of additional amorphous clathrate or grew crystalline clathrates. This analysis also allowed us to investigate whether the sI clathrate lattice could cross nucleate the sII clathrate, a phenomenon previously observed in the growth of methane and guest-free clathrates.[15,30]

A notable finding from this study is that crystalline clathrates can grow from amorphous nuclei. This is illustrated in Figures 2−4 that show initial amorphous and crystalline clathrate and the structures they grow from the solution at temperatures just below their respective melting points. All nuclei, whether crystalline or amorphous, eventually lead to the growth of crystalline and polycrystalline domains. The growth of clathrate cages around the nucleus was faster than the reorganization of the initial core of amorphous nuclei to form crystalline clathrates, thus an amorphous core remained encased within a crystalline (or polycrystalline) shell. Figure 3 shows that the smallest crystalline nucleus ($R \approx$ 10 Å) leads to the growth of polycrystalline domains, perhaps because the increased supercooling of the system (held at 240 K) with respect to both the bulk sI and sII phases. We note that the conditions of this study favor relatively fast growth of post critical nuclei, because there is no mass-transport

dx.doi.org/10.1021/ja201403q |J. Am. Chem. Soc. 2011, 133, 6458–6463

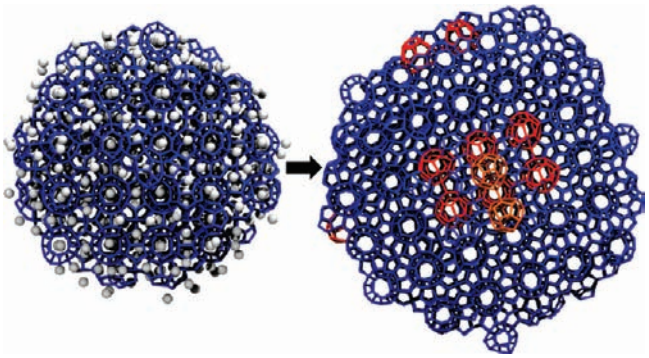

Figure 4. R = 30 Å sI nucleus at the beginning of the simulation (left) and after 52 ns of growth (right) at T = 270 K. The sI lattice (blue) is able to template the growth of sII (orange) through the $5^{12}6^3$ cages (red). The nucleus started out with 3406 water molecules belonging to cages in the sI structure. The final structure shown above has 7629 water molecules as part of a polyhedral cage, 90% of which were identified as being sI. For clarity, guest molecules (white balls) are not shown in the final structure.

limitation (the guest molecules have to cross a short path from the guest liquid slab to reach the nucleus; see the Abstract graphic). We expect that even if amorphous nuclei form first, favored by a lower free energy barrier at high supercooling, slow growth of these critical nuclei under conditions where the accessibility of guests to the growing surface is a limiting factor should lead to an increase in nuclei crystallinity already for small sizes, before they grow a macroscopic crystal phase.

Large sI crystalline nuclei grow sI clathrates, nevertheless we also observe cross-nucleation of the sII crystal from the sI core facilitated by the formation of $5^{12}6^3$ cages, as shown in Figure 4. Despite the sI or amorphous nature of the initial nuclei, all the systems eventually grow predominantly the sII structure, and not the most stable sI crystal. In this regard, this is different from the cross-nucleation from sI to sII in guest-free clathrates, where the sII structure is the most stable phase.[15] The relative stabilities of sI and sII in the methane-water model used in ref 30 are not known; nevertheless the results presented here demonstrate that cross-nucleation toward the least stable crystal is possible under conditions where the two crystals are more stable than the solution.

The cross nucleation of sII from sI, even though the sI crystal is thermodynamically more stable, attests to the important role of kinetic factors not only for the nucleation but also for the subsequent growth of the clathrates. Our finding is in agreement with experimental observations of methane hydrate formation in which the metastable sII structure preferentially forms at the onset, but later transforms into the stable sI polymorph.[31,32] The transformation of the kinetically favored metastable sII crystal into the stable sI lattice can take hours to days,[31,32] and is not observed in the time scale of the simulations. The very slow kinetics of the sII to sI ripening suggests that advanced sampling methods are necessary for its study through molecular simulations.

■ CONCLUSIONS AND OUTLOOK

We used molecular dynamics simulations with a very efficient force-field to investigate the thermodynamics, size and crystallinity of clathrate hydrate clusters of a small hydrophobic guest with properties intermediate between those of CH_4 and CO_2, and evaluate their potential as nuclei for the crystallization of clathrates. A main finding of this study is the relatively high stability of the amorphous solid clathrate phase, more stable than the water-guest solution for supercooling larger than 10%. The stability of the amorphous clathrate is key in favoring nucleation pathways that proceed, as previously reported for the crystallization of proteins, colloids and nanoparticles,[8−12,33,34] through amorphous intermediates.[6,7,14]

We determined the critical nucleus size for amorphous and crystalline clathrates as a function of temperature and found that it is well-described by the Gibbs−Thomson equation, from which we extract a liquid-crystal surface tension in excellent agreement to that determined from the experimental study of melting of CH_4 and CO_2 clathrates in nanopores. While for each temperature the size of the critical amorphous nuclei is predicted to be larger than the critical crystalline nuclei, our analysis based on tentative values of the liquid-amorphous clathrate surface tension suggest that, at high supercooling, the nucleation through amorphous clathrates could be kinetically favored by lower free energy barriers, thus explaining the results obtained in simulations at high driving force, where amorphous nuclei initiate the formation of clathrates.[4−6,14,25−28]

This study demonstrates that amorphous nuclei can grow crystalline clathrates, even under conditions where they do not ripen to crystalline nuclei before growing. This implies that the observation of macroscopic crystalline clathrates should not be used to rule out a mechanism of formation that proceeds through an amorphous clathrate intermediate. Most important, the cross-nucleation from the stable sI to the least stable sII crystal under conditions where the two are more stable than the solution reveals the importance of kinetic factors in the growth of clathrates. Recent work by Peters stresses the role of the diffusion tensor anisotropy on polymorph selection for the crystallization of a mixture of oppositely charged colloids.[35] It would be of interest to investigate whether the formation of sII is favored over the growth of sI by lower free energy barriers in the nucleation pathway or by purely dynamical effects.

An important and still not fully answered question is what is the highest temperature for which nucleation through amorphous clathrate nuclei is competitive with respect to the formation of smaller crystalline nuclei. The infrared spectra of clathrates formed from aqueous nanodroplets at 200 K show signatures that are not consistent with sI, sII or a combination of the two crystals,[36] suggesting that amorphous clathrates may have formed under those conditions. At low driving forces, outside of the region of stability for the amorphous clathrate, only crystalline nuclei could be stable. The critical radius of crystalline nuclei at the temperature of melting of bulk (i.e., infinite) amorphous clathrate is about 4 nm, thus large clathrate nuclei must be crystalline. Consistent with this prediction, Lehmkühler et al. identified CO_2 clathrate crystal clusters of about 20 nm diameter close to the water-CO_2 interface for conditions of relatively low driving force, that nevertheless do not grow macroscopic clathrates within the time scale of their experiments.[37] It is possible, however, that even at low driving force, density fluctuations of the guest molecules in solution that form a transient amorphous intermediate could facilitate the growth of crystalline clathrates. Enhanced sampling techniques are needed to determine in an unbiased way the actual pathways, free energy barriers and dynamical factors involved in the crystallization of clathrates at low driving force.

AUTHOR INFORMATION

Corresponding Author
Valeria.Molinero@utah.edu

ACKNOWLEDGMENT

We gratefully acknowledge support by the National Science Foundation through award CHE-1012651 and thank the Center of High Performance Computing of the University of Utah for allocation of computing time.

REFERENCES

(1) Sloan, E. D.; Koh, C. A. *Clathrate Hydrates of Natural Gases*; 3rd ed.; CRC Press/Taylor-Francis: Boca Raton, FL, 2007.
(2) Koh, C. A.; Sum, A. K.; Sloan, E. D. *J. Appl. Phys.* **2009**, *106*, 061101–14.
(3) Sum, A. K.; Koh, C. A.; Sloan, E. D. *Ind. Eng. Chem. Res.* **2009**, *48*, 7457–7465.
(4) Hawtin, R. W.; Quigley, D.; Rodger, P. M. *Phys. Chem. Chem. Phys.* **2008**, *10*, 4853–4864.
(5) Walsh, M.; Koh, C.; Sloan, E.; Sum, A.; Wu, D. *Science* **2009**, *326*, 1095.
(6) Jacobson, L. C.; Hujo, W.; Molinero, V. *J. Am. Chem. Soc.* **2010**, *132*, 11806–11811.
(7) Vatamanu, J.; Kusalik, P. G. *Phys. Chem. Chem. Phys.* **2010**, *12*, 15065–15072.
(8) Erdemir, D.; Lee, A. Y.; Myerson, A. S. *Acc. Chem. Res.* **2009**, *42*, 621–629.
(9) Whitelam, S. *J. Chem. Phys.* **2010**, *132*, 194901–5.
(10) Wolde, P. R. t.; Frenkel, D. *Science* **1997**, *277*, 1975–1978.
(11) Vekilov, P. G. *J. Cryst. Growth* **2005**, *275*, 65–76.
(12) Liu, H.; Kumar, S. K.; Douglas, J. F. *Phys. Rev. Lett.* **2009**, *103*, 018101.
(13) Jacobson, L. C.; Molinero, V. *J. Phys. Chem. B* **2010**, *114*, 7302–7311.
(14) Jacobson, L. C.; Hujo, W.; Molinero, V. *J. Phys. Chem. B* **2010**, *114*, 13796–13807.
(15) Jacobson, L. C.; Hujo, W.; Molinero, V. *J. Phys. Chem. B* **2009**, *113*, 10298–10307.
(16) Molinero, V.; Moore, E. B. *J. Phys. Chem. B* **2009**, *113*, 4008–4016.
(17) Plimpton, S. J. *J. Comput. Phys.* **1995**, *117*, 1–19.
(18) *Handbook of Chemistry and Physics*; CRC: Boca Raton, FL, 2000−2001; Vol. 81.
(19) Moore, E. B.; de la Llave, E.; Welke, K.; Scherlis, D. A.; Molinero, V. *Phys. Chem. Chem. Phys.* **2010**, *12*, 4127–4134.
(20) Petrov, O. V.; Furó, I. *Prog. Nucl. Magn. Reson. Spectrosc.* **2009**, *54*, 97–122.
(21) Jaehnert, S.; Vaca Chavez, F.; Schaumann, G. E.; Schreiber, A.; Schoenhoff, M.; Findenegg, G. H. *Phys. Chem. Chem. Phys.* **2008**, *10*, 6039–6051.
(22) Anderson, R.; Llamedo, M.; Tohidi, B.; Burgass, R. W. *J. Phys. Chem. B* **2003**, *107*, 3507–3514.
(23) Uchida, T.; Ebinuma, T.; Takeya, S.; Nagao, J.; Narita, H. *J. Phys. Chem. B* **2002**, *106*, 820–826.
(24) Kashchiev, D.; Firoozabadi, A. *J. Cryst. Growth* **2002**, *243*, 476–489.
(25) Liang, S.; Kusalik, P. G. *Chemical Science* **2011**, under review.
(26) Moon, C.; Taylor, P. C.; Rodger, P. M. *J. Am. Chem. Soc.* **2003**, *125*, 4706–4707.
(27) Zhang, J.; Hawtin, R. W.; Yang, Y.; Nakagava, E.; Rivero, M.; Choi, S. K.; Rodger, P. M. *J. Phys. Chem. B* **2008**, *112*, 10608–10618.
(28) Moon, C.; Hawtin, R. W.; Rodger, P. M. *Faraday Discuss.* **2007**, *136*, 367–382.
(29) Jacobson, L. C.; Molinero, V. "Order parameters for the multistep crystallization of clathrate hydrates", in preparation.
(30) Vatamanu, J.; Kusalik, P. G. *J. Am. Chem. Soc.* **2006**, *128*, 15588–15589.
(31) Staykova, D. K.; Kuhs, W. F.; Salamatin, A. N.; Hansen, T. *J. Phys. Chem. B* **2003**, *107*, 10299–10311.
(32) Murshed, M. M.; Kuhs, W. F. *J. Phys. Chem. B* **2009**, *113*, 5172–5180.
(33) Savage, J. R.; Dinsmore, A. D. *Phys. Rev. Lett.* **2009**, 102.
(34) Duff, N.; Peters, B. *J. Chem. Phys.* **2009**, *131*, 184101.
(35) Peters, B. *J. Chem. Phys.* **2009**, *131*, 244103.
(36) Devlin, J. P.; Monreal, I. A. *Chem. Phys. Lett.* **2010**, *492*, 1–8.
(37) Lehmkühler, F.; Paulus, M.; Sternemann, C.; Lietz, D.; Venturini, F.; Gutt, C.; Tolan, M. *J. Am. Chem. Soc.* **2009**, *131*, 585–589.